

Mechanics of Silicon Nanowires: Size-Dependent Elasticity From First Principles

Robert E. Rudd and Byeongchan Lee

Lawrence Livermore National Laboratory
University of California, L-045
Livermore, California 94551 USA

ABSTRACT

We review our recent work on the mechanics of silicon nanowires based on first-principles density functional theory (DFT) calculations. We focus especially on the size dependence of the Young's modulus, but also comment on the size dependence of the residual stress and the equilibrium length of the hydrogen-passivated Si nanowires. We compare these results to prior results from classical molecular dynamics based on empirical potentials.

Keywords: nanowire, Young's modulus, density functional theory, size effect, surface stress

1 THE MECHANICS OF NANOWIRES

Nanowires are being studied as mechanical components for a range of potential devices. Clamped at one or both ends, they can act as mechanical resonators for applications ranging from high frequency oscillators and filters [1] to q-bits in quantum computers [2], [3]. As the device size is reduced, the frequency of the fundamental mode increases. Further miniaturization is then a way to increase the operating frequency of the oscillator. This increase in frequency can be quite desirable, provided other properties such as the quality factor of the resonator do not degrade too much. For example, the frequency of a mechanical q-bit determines the energy of its quantum state, and higher frequencies are less susceptible to decoherence from thermal fluctuations.

The basic theory governing the oscillations of a mechanical resonator is based on continuum elasticity. The theory is certainly valid for sufficiently large resonators where the materials are continuous media to a very good approximation. In limit that the oscillating beam becomes a chain of atoms, the nature of the bonding is quite different than the bulk, and while the behavior may still be elastic, the elastic properties are expected to be significantly altered. In between, there is a range of beam sizes in which the beams are three dimensional, but the properties of the atoms on the surface may be quite different than the bulk. As the beam is miniaturized, the surfaces have an increasingly strong influence on the behavior of the beam.

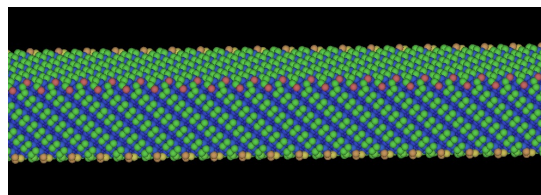


Figure 1: (Color) Image of the 3-nm silicon nanowire showing the 2×1 $\{100\}$ dimer reconstruction for the Stillinger-Weber potential. Calculation of the Young's modulus involves expanding the periodic box in the wire's longitudinal direction, allowing the wire to relax to mechanical equilibrium in the transverse directions, and calculating the resulting axial stress. Each sphere represents a Si atom, colored according to that atom's energy at zero temperature.

The size dependence of nanowire mechanical properties has been attributed largely to these surface effects [4]–[7], caused specifically by surface stress and surface elastic constants. The properties of surfaces are different from those of the bulk due to the structural changes coming from the relatively unconstrained structure at the surface and modifications of the bonding environment seen in changes in the bond order. The preferred interatomic spacing at the surface may be different than that of the bulk, and the strain to form a coherent interface results in the surface stress. Similarly the changes in the atomic interactions at the surface can result in local changes in the elastic properties expressed surface elastic constants.

In this article, we review results on the size dependence of the nanowire mechanical properties, especially the Young's modulus. We have recently conducted what is, to the best of our knowledge, the first systematic study based on first-principles calculations of the Young's modulus of any type of nanowire [8], [9]. We have thus far studied hydrogen-passivated Si $\langle 001 \rangle$ nanowires, finding that the nanowires are less stiff as their size decreases, and that the form of the size dependence is well described by existing theories. We compare to earlier calculations of the size-dependent mechanical properties predicted by atomistic simulations of nanowires using classical empirical potentials, as shown in Fig. 1.

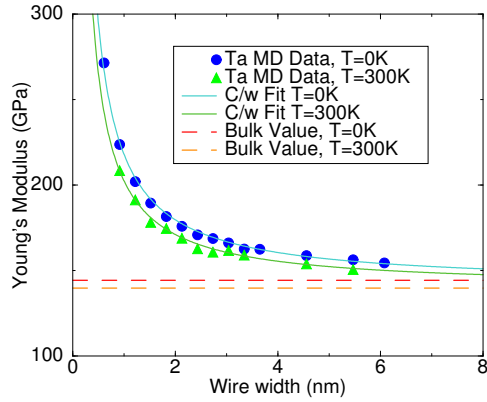


Figure 2: The Young's modulus of tantalum nanowires calculated from molecular dynamics at absolute zero and room temperature using the Finnis-Sinclair potential [11]. The wire orientation is $\langle 001 \rangle$ with $\{100\}$ surfaces. Both of the curves show a size effect in which the Young's modulus increases (stiffens) as the size is reduced, with thermal softening at finite temperature.

2 PREDICTIONS OF EMPIRICAL ATOMISTICS

We have performed classical molecular dynamics simulations in order to study the elastic behavior of silicon nanowires [10], [11]. These calculations are based on empirical many-body interatomic potentials, specifically the Stillinger-Weber (SW) potential [12] for silicon and the Finnis-Sinclair potential [14], [15] for tantalum. Much of this work was done some time ago, and there have been similar results published by other groups, including one study using an empirical tight-binding method [16] that, albeit not *ab initio*, is more powerful than the classical potentials. Our purpose in reporting the empirical atomistic results here is to motivate and compare to the first-principles calculations described below.

These simulations were conducted on a system of atoms in a monatomic single crystal, apart from the surfaces, aligned such that the longitudinal axis of the simulated nanowire is the $\langle 001 \rangle$ crystal axis. This orientation is suitable for etched systems like NEMS. Nanowires typically grow with other orientations [17]. The nanowire spans two periodic boundaries of the simulation box, surrounded by vacuum in the transverse directions. The system was brought to mechanical and thermal equilibrium. The simulation box was expanded to stretch the nanowire, allowing the wire to relax either adiabatically at finite temperature or by steepest descent at zero temperature. The resulting stress-strain curve was fit to a fifth-order polynomial in order to calculate the Young's modulus. A typical result for the size dependence of a metal nanowire is depicted in the Young's modulus of

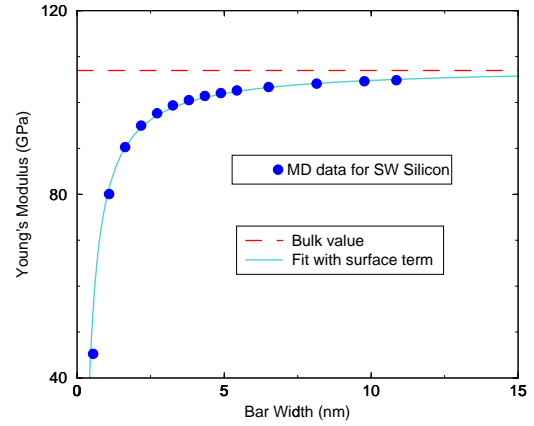


Figure 3: The Young's modulus of Si nanowires calculated from molecular dynamics at zero temperature using the Stillinger-Weber (SW) potential. The wire orientation is $\langle 001 \rangle$ with dimer reconstructed $\{100\}$ surfaces. The size effect has a different sign from that of tantalum shown in Fig. 2.

tantalum nanowires shown in Fig. 2 [11] calculated using the Finnis-Sinclair potential [14], [15]. The modulus increases as the size is reduced, both at zero and room temperature. The principal temperature dependence is the thermal softening of the bulk value of the Young's modulus although there is a temperature dependence to the coefficient of the size-dependent term as well.

The size dependence of bare Si $\langle 001 \rangle$ nanowires is shown in Fig. 3, based on atomistic calculations with the Stillinger-Weber interatomic potential for silicon [12]. The zero temperature case is plotted; the effect of finite temperature is analogous to that of tantalum. A size effect is seen in both cases. As in the tantalum example, the data points are fit well by the solid curves of the form $E_0 + C/w$, where E_0 is the bulk value of the Young's modulus and w is the width of the nanowire. For the current purposes, C is a fitting constant. In principle it is related to the surface elastic constants.

One of the more striking aspects of Fig. 3 is that the sign of the surface effect is different than that for the metal in Fig. 2. The SW beams soften and the Ta beams stiffen as the size is reduced. It is not surprising that the magnitude of the effect would be different in the two cases. Both potentials include many-body forces, but the Finnis-Sinclair potential includes an environmental dependence that is absent from the Stillinger-Weber potential. Neither potential is fit to nanowire data, although the surface structures and energies calculated with the two potentials are generally reasonable and comparable [13]. It is an interesting question then whether the Stillinger-Weber potential is realistic and accurate enough for meaningful calculations. Lacking suitable experimental data, we turn to first-principles

calculations to make this assessment.

3 FIRST-PRINCIPLES CALCULATIONS

We have calculated the Young's modulus and other mechanical properties of silicon nanowires using first-principles density functional theory (DFT) at absolute zero temperature [8], [9]. Specifically, we have employed the Vienna Ab-initio Simulation Package (VASP) using the projector augmented-wave method [18], [19] within the generalized gradient approximation (GGA) [20]. The energy cutoff for the plane-wave expansion is 29.34 Ry and higher, and six points in the one-dimensional irreducible Brillouin zone are used for k -point sampling. Each supercell is periodic, is one Si cubic unit cell long along the hydrogen-passivated nanowire and has more than 10 Å vacuum space in the transverse directions. Computational resources have limited the size of the nanowires we can study. The largest nanowire, 3.92 nm in diameter, consisted of 405 Si atoms and 100 H atoms.

The nanowire simulations were constructed in a periodic box, aligned much as in the empirical atomistic calculations described above. The Si atoms were placed at the sites of a perfect Si diamond-cubic crystal, and H atoms were placed above the surfaces, two per Si atom on the {100} surfaces and one per Si atom on the {110} surfaces. The dihydride Si {100} surface is known to be the ground state at low temperatures [21]. The shape of the nanowires was taken to be the Wulff shape corresponding to the surface energies for bare, reconstructed Si {100} and {110} surfaces. The bare energies were used in order to create structures suitable for comparison with bare wires, a topic of future research.

For each strain, the box dimensions were adjusted and the atoms in the nanowire were relaxed using conjugate gradient to a residual force of less than 2-10 meV/Å. The details of the calculations are given in Ref. [9]. The relaxed total energies were used to calculate the physical observables: the residual stress, the equilibrium length and the Young's modulus.

3.1 Residual Stress and Equilibrium Length

The axial stress of the nanowire constrained to be at the length corresponding to the unstrained bulk crystal is an estimate of the residual stress that would be present in a nanowire etched from a substrate with the ends still attached to that substrate. The axial stress is determined from the derivative of the fit to the total energy as a function of strain [8]

$$\sigma_{zz}(L_0) = V^{-1} \partial U / \partial \epsilon_{zz} |_0 \quad (1)$$

where U is the DFT total energy. It turns out that a parabolic fit describes the total energy very well for the

small strains of up to a few percent that we used, so the residual stress is also equal in this approximation to the Young's modulus times the equilibrium strain. In any case, we have examined the size dependence of the residual stress and found that it is described well by the form (see Ref. [8])

$$\sigma_{zz}(L_0) = \sigma_{zz}(core) + \frac{1}{A} \sum_i \tau_{zz}^{(i)} w_i \quad (2)$$

where A is the cross-sectional area, w_i is the width, and $\tau_{zz}^{(i)}$ is the longitudinal surface stress, of facet i . The size dependence is thus proportional to the surface area to volume ratio. The equilibrium elongation of the larger wires also shows this scaling (see Ref. [8] for details).

3.2 Young's Modulus

The Young's modulus is calculated from the second derivative of the relaxed total energy as a function of strain. The results are shown in Fig. 4. The square symbols denote the first-principles results. The Young's modulus softens as the size of the nanowire is reduced, as was seen for the Stillinger-Weber atomistic calculations above. The + signs denote the results of a continuum model parameterized with DFT data derived entirely from bulk and surface slab calculations, rather than the more computationally expensive explicit nanowire geometry. The dashed curve denotes the results of a fit to published molecular statics calculations based on the Stillinger-Weber potential [6] for 1×1 Si {100} wires. The solid curve represents a fit to $E_0 + C/w$ where E_0 is the Young's modulus of the bulk crystal and w is the width of the nanowire. Even though the 1×1 {100} surface is not the ground state and the calculation is therefore contrived, it may be a better analog of the H passivated wire than the more realistic 2×1 bare wires of Figs. 1 and 3.

The comparison of the Young's modulus of a hydrogen-passivated Si nanowire calculated with DFT to the Young's modulus of a bare Si nanowire calculated with empirical atomistics is not a direct comparison; nevertheless, it is interesting that the Stillinger-Weber potential is reasonably close to the first-principles result. It does not contain any physics characteristic of the surface, such as a change in the bond character. Of course, the effect of the H passivation is to mitigate some of the environmental dependence that more sophisticated potentials are designed to capture. We need the results of DFT calculations for bare wires to make a direct comparison.

4 CONCLUSION AND OUTLOOK

We have studied the mechanics of Si nanowires using first-principles techniques. The results on the size dependence of the Young's modulus are consistent with the dominant contribution coming from surface effects,

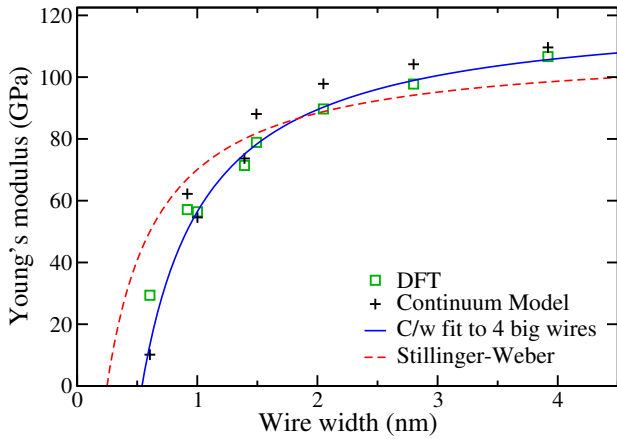


Figure 4: The Young's modulus of hydrogen-passivated Si $\langle 001 \rangle$ nanowires calculated from first principles in DFT [8]. The square symbols denote the DFT results. For comparison three other values are plotted, as described in the text.

as verified from comparison to a continuum model parameterized with data from first principles calculations of bulk and slab systems. Recently, there have been increasing experimental efforts to measure the size dependence of the nanowire Young's modulus for several materials [22]–[27]. The vast majority of these nanowires are much larger than the ones we have studied. Computational limitations prevent us from calculating the modulus of the larger wires, but scaling up from our results would suggest that the effect would be negligible for hydrogen-passivated Si $\langle 001 \rangle$ larger than 10 nm.

There are many questions that remain open regarding the nanowire mechanics. There are some hints that effects from sources other than surfaces are important in the smallest wires we have studied. The hydrogen-passivated surfaces are among the most benign possible, so it is natural to ask whether the threshold for these anomalies occurs at a larger size for other types of surfaces. The exact nature of these effects is unknown. Even for the more conventional surface effects, we still do not have an understanding of the physics that is sufficiently powerful to allow us to derive an effective interatomic potential that reproduces the first-principles behavior. Some efforts have begun along these lines [28], but clearly much more is needed in terms of theory, development and validation.

Acknowledgments

We are grateful to Livermore Computing for extensive supercomputer resources on MCR and Thunder. This work was performed under the auspices of the U.S. Department of Energy by the University of California, Lawrence Livermore National Laboratory, under Contract No. W-7405-Eng-48. R.E.R. gratefully acknowledges the support of the National Science Foundation

through NIRT Grant Award No. CMS-0404031.

REFERENCES

- [1] A. N. Cleland and M. L. Roukes, *Appl. Phys. Lett.* **69**, 2653, 1996.
- [2] A. N. Cleland and M. R. Geller, *Phys. Rev. Lett.* **93**, 070501, 2004.
- [3] M. Blencowe, *Phys. Rep.* **395**, 159, 2004.
- [4] J. W. Cahn, *Acta Metall.* **28**, 1333, 1980.
- [5] J. Q. Broughton, C. A. Meli, P. Vashishta, and R. K. Kalia, *Phys. Rev. B* **56**, 611, 1997.
- [6] R. E. Miller and V. B. Shenoy, *Nanotech.* **11**, 139, 2000.
- [7] H. Liang, M. Upmanyu, and H. Huang, *Phys. Rev. B* **71**, 241403(R), 2005.
- [8] B. Lee and R. E. Rudd, *Phys. Rev. B* **75**, 041305(R), 2007.
- [9] B. Lee and R. E. Rudd, submitted to *Phys. Rev. B*. <http://www.arxiv.org/abs/cond-mat/0702531>
- [10] R. E. Rudd and J. Q. Broughton, *J. Mod. Sim. Microsys.* **1**, 29, 1999.
- [11] R. E. Rudd, *Int. J. Multiscale Comp. Eng.* **2**, 203, 2004.
- [12] F. H. Stillinger and T. A. Weber, *Phys. Rev. B* **31**, 5262, 1985.
- [13] H. Balamane, T. Halicioglu, and W. A. Tiller, *Phys. Rev. B* **46**, 2250, 1992.
- [14] M. Finnis and J. Sinclair, *Philos. Mag. A* **50**, 45, 1984.
- [15] G. J. Ackland and R. Thetford, *Phil. Mag. A*, **56**, 15, 1987.
- [16] D. E. Segall, S. Ismail-Beigi, and T. A. Arias, *Phys. Rev. B* **65**, 214109, 2002.
- [17] C. M. Lieber, *MRS Bull.* **28**, 486, 2003.
- [18] P. E. Blöchl, *Phys. Rev. B* **50**, 17953, 1994.
- [19] G. Kresse and D. Joubert, *Phys. Rev. B* **59**, 1758, 1999.
- [20] J. P. Perdew, K. Burke, and M. Ernzerhof, *Phys. Rev. Lett.* **77**, 3865, 1996.
- [21] S. Ciraci and I. P. Batra, *Surf. Sci.* **178**, 80 (1986).
- [22] E. W. Wong, P. E. Sheehan, and C. M. Lieber, *Science* **277**, 1971, 1997.
- [23] S. Cuenot, C. Fretigny, S. Demoustier-Champagne, and B. Nysten, *Phys. Rev. B* **69**, 165410, 2004.
- [24] C. Q. Chen, Y. Shi, Y. S. Zhang, J. Zhu, and Y. J. Yan, *Phys. Rev. Lett.* **96**, 075505, 2006.
- [25] X. Q. Chen, S. L. Zhang, G. J. Wagner, W. Q. Ding, and R. S. Ruoff, *J. Appl. Phys.* **95**, 4823, 2004.
- [26] T. Kizuka, Y. Takatani, K. Asaka, and R. Yoshizaki, *Phys. Rev. B* **72**, 035333, 2005.
- [27] A. San Paulo *et al.*, *Appl. Phys. Lett.* **87**, 053111, 2005.
- [28] B. Lee and K. Cho, *Surf. Sci.* **600**, 1982, 2006.